

Oscillatory exchange coupling in Co/Cu(111) superlattices

A. Schreyer and K. Bröhl

Experimentalphysik IV, Ruhr-Universität Bochum, 44780 Bochum, Federal Republic of Germany

J. F. Ankner and C. F. Majkrzak

National Institute of Standards and Technology, Gaithersburg, Maryland 20899

Th. Zeidler, P. Bödeker, N. Metoki, and H. Zabel

Experimentalphysik IV, Ruhr-Universität Bochum, 44780 Bochum, Federal Republic of Germany

(Received 19 January 1993; revised manuscript received 4 May 1993)

By probing the magnetization profile of high-quality molecular-beam-epitaxy-grown Co/Cu(111) superlattices with spin-polarized neutron reflectivity (SPNR), we have observed a coherent antiferromagnetic spin structure and confirm that this coupling behavior sensitively depends on the Cu spacer thicknesses. We present magneto-optical Kerr-effect data from which the oscillation period of the exchange coupling can be determined to be about 9 Å, consistent with theory and the SPNR data. With these results we confirm the existence of an oscillatory exchange coupling in this controversial system.

The discovery of an exchange coupling between magnetic layers, which oscillates between ferromagnetic (FM) and antiferromagnetic (AF) as a function of spacer thickness in layered magnetic rare-earth (RE)¹ and transition-metal^{2,3} structures has initiated major activities both in fundamental and applied research. This oscillatory exchange coupling has since been observed in a large number of systems.^{4,5} For the RE materials this coupling behavior has been attributed to the Ruderman-Kittel-Kasuya-Yosida (RKKY) interaction.^{1,5} Similarly, it was shown that also in the case of transition metals the coupling can be understood in terms of this mechanism⁶ by taking into account the topological properties of the Fermi surface of the spacer material.^{7,8} According to Refs. 7 and 8 the coupling is mediated by one or more nesting vectors parallel to the respective growth direction, which connect parts of the Fermi surface with antiparallel Fermi velocities. Consequently the coupling behavior depends sensitively on the growth direction and on details of the Fermi surface. Since fcc Co/Cu can be grown epitaxially in various orientations it has been regarded as a model system for the test of these theoretical predictions.

Whereas Co/Cu(100) was one of the first systems in which AF exchange coupling had been demonstrated⁹ a dispute erupted over its existence in Co/Cu(111) for which an oscillation period of 4.5 ML (~ 9 Å) had been predicted.⁷ After the first report of oscillatory exchange coupling in sputtered Co/Cu(111) multilayers³ with a rather weak (111) texture,^{11,12} the absence of any convincing evidence for AF spin alignment in molecular-beam-epitaxy- (MBE) grown highly textured Co/Cu(111) trilayers was reported.¹² In Ref. 12 it was suggested that the AF coupling in the sputtered multilayers could have been mediated by minority components of grains which were oriented at or near (100) instead of (111). Since then a number of groups have reported positive evidence for the existence of AF exchange coupling in

Co/Cu(111) grown by MBE methods for a copper thickness of $t_{\text{Cu}}^{\text{AF}}(1) \approx 9$ Å. These conclusions were drawn from techniques which probe macroscopic properties like the magneto-optical Kerr effect (MOKE),¹⁰ torsion oscillation magnetometry,¹³ superconducting quantum interference device (SQUID) magnetometry,¹⁴ and magnetoresistance (MR) measurements.¹⁴⁻¹⁶ Nevertheless, in none of these reports has convincing evidence for the existence of the second regime of AF coupling at $t_{\text{Cu}}^{\text{AF}}(2) \approx 19$ Å been provided so far, as would be expected from the nature of an oscillatory coupling for Co/Cu(111).⁷

In this paper we present spin polarized neutron reflectivity (SPNR) data on high-quality MBE-grown Co/Cu(111) superlattices which, since SPNR directly probes the magnetization profile, unambiguously proves the existence of a coherent AF order for both $t_{\text{Cu}}^{\text{AF}}(1)$ and $t_{\text{Cu}}^{\text{AF}}(2)$ in this system. Furthermore we demonstrate the absence of AF order for an intermediate t_{Cu} . We correlate these results with MOKE data which show a distinct oscillation of the saturation fields with three maxima, again indicating an oscillatory exchange coupling in Co/Cu(111).

Using a commercial two-chamber MBE system (Riber EVA 32) the samples were grown on 25×25 mm² Al₂O₃(11 $\bar{2}$ 0) substrates at pressures below 2×10^{-8} Pa during evaporation.¹⁷ First, a 50–100-Å Nb(110) buffer was deposited with a rate of 0.5 Å/s at a substrate temperature of 900 °C. As shown by *in situ* reflection high-energy electron diffraction (RHEED), annealing at 950 °C for 20 min increased the smoothness of the Nb surface considerably.¹⁸ To maximize the degree of crystallinity, the growth of the superlattice was started with a Cu seed layer at an optimized substrate temperature of 375 °C. By continuing the growth at RT the interface diffusion of the subsequent alternating Co and Cu layers was minimized. The growth rates were 0.1 Å/s and 0.07 Å/s for Co and Cu, respectively.

The samples were thoroughly characterized chemically

by x-ray fluorescence and structurally by x-ray low-angle reflectivity, high-angle Bragg scattering, and grazing incidence diffraction techniques as detailed elsewhere.¹⁷ These measurements confirmed the high quality of the samples with an fcc structure of both Cu and Co (bulk Co is hcp at RT). The superlattices have a very strong (111) texture in the growth direction which is evidenced by the very small full width at half-maximum (FWHM) of the out-of-plane rocking curves of only 0.02°–0.1°. No (100) or (110) peaks were observed. Due to a misfit of the lattice constants of Co and Cu of about 2%, the superlattices are strained with coherent in-plane matching and corresponding out-of-plane Poisson response.¹⁷ In Fig. 1 typical x-ray data are shown together with theoretical fits plotted as a function of normal scattering vector $|Q| = (4\pi/\lambda) \sin \theta$ for x rays of wavelength $\lambda = 1.542 \text{ \AA}$ incident at angle θ onto the sample surface. Both high- and low-angle data show strong superlattice peaks and finite thickness oscillations. In the high-angle data these oscillations indicate a coherence length along the growth direction extending over 80% of the total film thickness. The broad peak around 2.75 \AA^{-1} is due to the Nb buffer.

From the fits to the data a roughness, defined as the rms deviation $\sqrt{\langle z^2 \rangle}$ from the ideal interface, of 4 \AA (high-angle scattering) and 7 \AA (low-angle reflectivity) of the Co/Cu interfaces was found. Therefore, despite the care taken during sample growth, a certain degree of intermixing of the layers cannot be ruled out. The difference between the high- and low-angle roughnesses is discussed in Ref. 17. No fluctuation of the individual t_{Cu} had to be assumed to quantitatively explain the data.

The SPNR measurements were carried out at the National Institute of Standards and Technology in Gaithersburg/USA on the reflectometer BT-7.¹⁹ A monochromated thermal neutron beam was polarized and analyzed by Fe/Si supermirrors. $\theta/2\theta$ specular reflectivity scans were performed for all four cross sections $\sigma(+, +)$, $\sigma(-, -)$, $\sigma(+, -)$, and $\sigma(-, +)$, where + (–) indicates the neutron spin state parallel (antiparallel) to an applied field in front of and behind the sample, re-

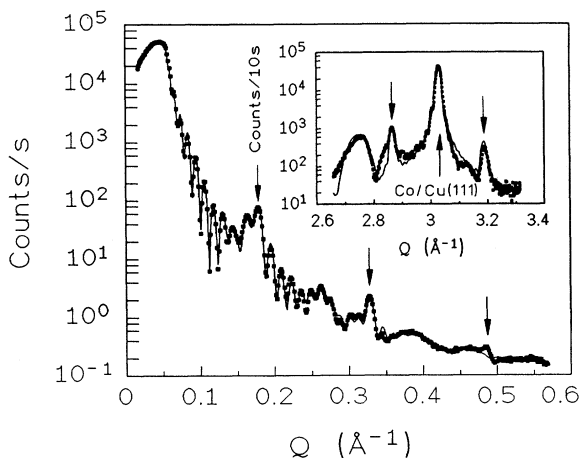


FIG. 1. Low- and high-angle x-ray data of the superlattice $[14.1 \text{ \AA} \text{ Co}/24.8 \text{ \AA} \text{ Cu}]_{10}$ together with theoretical fits (solid lines). The superlattice peaks are indicated by arrows. For more details see text.

spectively. The first two non-spin-flip (NSF) cross sections contain information on the nuclear structure and on the sample in-plane spins parallel and antiparallel to the applied field, respectively. The two spin-flip (SF) cross sections, on the other hand, exclusively yield magnetic information on the in-plane spins normal to the applied field¹⁹ (see inset in Fig. 2). Further details about the application of SPNR with polarization analysis are described in Ref. 20. Diffuse scattering and background were measured by off-specular $(\theta - \delta\theta)/2\theta$ scans with a small offset $\delta\theta$. To force the AF coupled spins into a spin flop state with the moments parallel to the SF axis the samples were magnetized in a field of 300–700 Oe parallel to the NSF axis before starting the scans. During the measurements a small guide field of 14 Oe was applied to prevent depolarization of the neutrons.

Magnetic hysteresis curves were measured up to 5 kOe

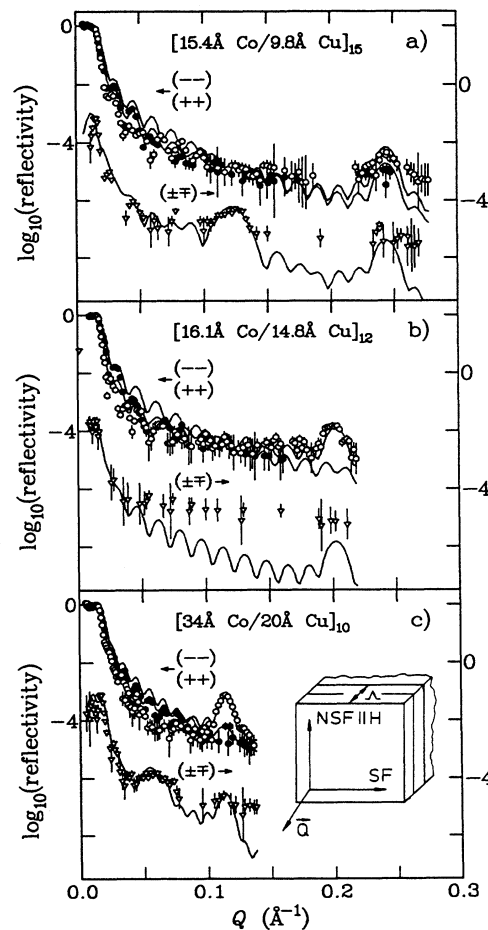


FIG. 2. Specular four cross-section SPNR data for three superlattices with $t_{\text{Cu}}^{\text{AFM}}(1)$ (a), $t_{\text{Cu}}^{\text{AFM}}(2)$ (c), and for an intermediate t_{Cu} (b) together with model calculations (solid lines). The data have been corrected for the efficiencies of the polarizing elements and the geometrical effect of the finite beam width. To obtain the true specular reflectivity the off-specular data were subtracted leaving some Q regions without specular intensity. The inset schematically shows a superlattice of period Λ with the applied field direction, the NSF and SF axis, and the scattering geometry used. For more details see text.

by MOKE in the longitudinal geometry with the external field parallel to the film plane.²¹ The existence of a magnetic in-plane anisotropy of the superlattices was ruled out by rotating the samples around an axis perpendicular to the film plane by a few degrees between subsequent measurements. In addition, the polar geometry with the external field perpendicular to the film plane was used to confirm that the magnetic moments had no out-of-plane component.

Figure 2 shows specular SPNR data together with model calculations (solid lines) for the four spin cross sections described above for three different superlattices plotted as a function of $|Q|$. The open circles represent NSF $(-, -)$, the closed circles NSF $(+, +)$, and the inverted triangles the sum of the SF $(+, -)$ and $(-, +)$ data, shifted downwards by two orders of magnitude relative to the NSF data. The SF cross sections are equal in this experiment and were added to improve the counting statistics. All NSF $(-, -)$ data sets show a regime of total external reflection up to Q_C^{NSF} at low- Q , finite-thickness oscillations related to the overall thickness of the superlattice and the first superlattice peak at $Q^{\text{SL}} = \sqrt{(2\pi/\Lambda)^2 + (Q_C^{\text{NSF}})^2}$, corresponding to the structural superlattice period $\Lambda = t_{\text{Co}} + t_{\text{Cu}}$. The NSF $(+, +)$ and SF data, on the other hand, exhibit weak or no superlattice peaks at Q^{SL} . As confirmed by the model calculations, this feature can only be explained as a consequence of at least a major part of the Co moments being aligned parallel to the initially applied field along the NSF axis. This leads to a lack of contrast between Co and Cu for the NSF $(+, +)$ cross sections. Consequently, at least a major part of the sample area must be FM coupled in all samples, since in this case magnetic and nuclear periodicity are equal, leading to the observed splitting of the NSF cross sections at Q^{SL} . Whereas in Fig. 2(b) no peak in the SF scattering is observed, the scans shown in Figs. 2(a) and 2(c) both clearly exhibit a peak at the respective half-order nuclear peak position, corresponding to twice the nuclear periodicity. Therefore these data unambiguously prove that the samples with $t_{\text{Cu}} = 9.8 \text{ \AA}$ and with $t_{\text{Cu}} = 20 \text{ \AA}$ contain coherent spin structures, which are consistent with an AF coupling between the Co layers. Since the SF cross sections contain information solely on the components of the Co moments which are parallel to the SF axis, the AF coupled regions have been forced into the spin flop state by the initially applied field. The fact that the sample with $t_{\text{Cu}} = 14.8 \text{ \AA}$ [Fig. 2(b)] does not exhibit a half-order peak confirms the spacer thickness dependence expected for an oscillatory exchange coupling.

In the inset of Fig. 3 the MOKE hysteresis curve of the AF sample of Fig. 2(a) is shown. No obvious sign of AF coupling, like the collapse of the Kerr rotation below a certain critical field is observed at first sight. Instead, for all t_{Cu} the hysteresis curves exhibit a large remanence, again indicative of a major ferromagnetic component in all samples. On the other hand, when the saturation field is plotted versus t_{Cu} , pronounced maxima around $t_{\text{Cu}} = 10 \text{ \AA}$, $t_{\text{Cu}} = 19 \text{ \AA}$, and $t_{\text{Cu}} = 28 \text{ \AA}$ are observed, as can be seen from Fig. 3. As indicated by the arrows in Fig.

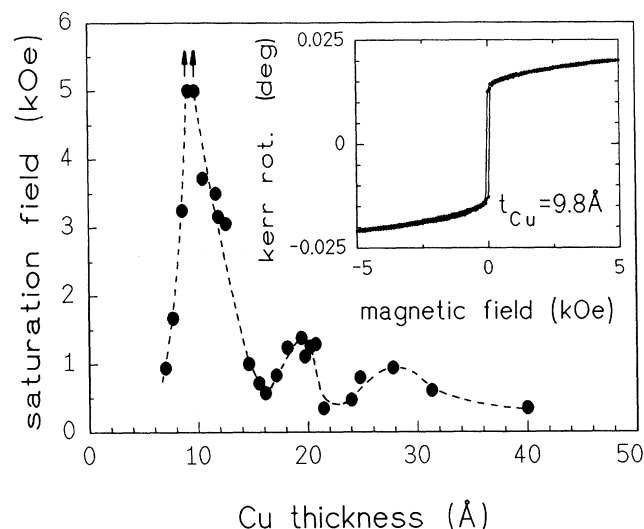


FIG. 3. Saturation fields determined from MOKE hysteresis curves from a series of Co/Cu superlattices as a function of t_{Cu} with the dashed line as a guide to the eye. The inset shows one of the two hysteresis curves which were not saturated at 5 kOe (as indicated by the arrows).

3 the two samples with maximum saturation field were not saturated at 5 kOe (see inset). The three maxima of the saturation field correspond to the external fields required to align the spins in the AF components in the respective samples. The first two AF regions have been verified by SPNR. The form of the hysteresis curves can be understood from the absence of an in-plane anisotropy in these samples, which allows for a gradual alignment of the Co spins with increasing field. From these MOKE results we actually infer evidence for a third AF coupling region around 28 \AA . Using the same relation as in Ref. 10 the AF coupling strengths J_{111} are estimated to be > 0.54 , 0.15 , and 0.10 mJ/m^2 for the first, second, and third maxima of the saturation field, respectively.

The AF domain fractions needed to reproduce the SF half-order peaks in the specular SPNR model curves were 25% and 15% for Figs. 2(a) and 2(c), respectively. These results coincide well with estimates of the AF fraction from the MOKE curves. Details on the model calculations and the assignment of FM and AF domain populations including a consideration of off-specular scattering will be discussed elsewhere.²²

Regarding the existence of a nonzero remanence and a maximum of the saturation fields for $t_{\text{Cu}}^{\text{AF}}(1)$, our magnetometry results on MBE-grown Co/Cu(111) are consistent with those published earlier.^{10,13-15} However, we find a much smaller oscillation period than the only other one reported¹³ for MBE-grown samples. Our result is close to the initially reported period of 10 \AA (Ref. 3) for the sputtered superlattices.

Our experimental result of an oscillatory exchange coupling in Co/Cu(111) with an oscillation period of about 9 \AA agrees well with the theoretical prediction by Bruno and Chappert.^{7,8} They have also pointed out that, due

to an angle γ of about 65° between the corresponding nesting vector and the Fermi velocities, the exchange coupling in Co/Cu(111) is much more sensitive to the effects of strain and interface roughness than in Co/Cu(100) with $\gamma = 0^\circ$.⁸ This result could explain, in part, the initial experimental difficulties encountered in the search for oscillatory exchange coupling in Co/Cu(111) and the observed FM components. Furthermore, it has been pointed out that local thinning of the Cu interlayers or pinholes could be responsible for the FM coupling component which has been observed in this work and in all experiments published earlier^{10,13-15} on MBE-grown samples. More detailed studies about the growth and structure of the Co/Cu(111) system are needed.

In conclusion we have observed an oscillation between coherent AF and FM spin structures in Co/Cu(111) superlattices as a function of t_{Cu} by SPNR, consistent with a distinct oscillation in the MOKE saturation fields. Not only the phase but also the period of the oscillatory exchange coupling has been determined in MBE-grown Co/Cu(111) samples, confirming its existence in this controversial system consistent with theory. Nevertheless

the origin of the FM component in MBE-grown samples remains yet to be clarified.

Note added in proof. We recently received a manuscript by Dupas *et al.*²³ who confirmed our results by the observation of an oscillatory MR with the same period. The observed amplitudes also indicate the presence of a major FM component. Very recent scanning-tunneling-microscope studies indicate that the observed FM component could result from Co bridges across noncoalesced Cu interlayers.²⁴ This mechanism is discussed in Ref. 13 in more detail.

We gratefully acknowledge discussions with J. Borchers, R. Coehoorn, and P. Grünberg as well as technical help by J. Podschwadek and W. Oswald. The work in Bochum was supported by the Deutsche Forschungsgemeinschaft through SFB 166 and the Bundesministerium für Forschung und Technologie through Grant No. 03-ZA3BOC. Furthermore, we would like to acknowledge travel support from the North Atlantic Treaty Organization through Grant No. CRG 901064.

-
- ¹C.F. Majkrzak *et al.*, Phys. Rev. Lett. **56**, 2700 (1986).
²S.S.P. Parkin, N. More, and K.P. Roche, Phys. Rev. Lett. **64**, 2304 (1990); S. Demokritov, J.A. Wolf, and P. Grünberg, Europhys. Lett. **15**, 881 (1991).
³S.S.P. Parkin, R. Bhadra, and K.P. Roche, Phys. Rev. Lett. **66**, 2152 (1991).
⁴S.S.P. Parkin, Phys. Rev. Lett. **67**, 3598 (1991).
⁵C.F. Majkrzak *et al.*, Adv. Phys. **40**, 99 (1991).
⁶See, for example, R. Coehoorn, Phys. Rev. B **44**, 9331 (1991).
⁷P. Bruno and C. Chappert, Phys. Rev. Lett. **67**, 1602 (1991).
⁸P. Bruno and C. Chappert, Phys. Rev. B **46**, 261 (1992).
⁹A. Cebollada *et al.*, Phys. Rev. B **39**, 9726 (1989).
¹⁰M.T. Johnson *et al.*, Phys. Rev. Lett. **69**, 969 (1992).
¹¹S.S.P. Parkin, in *Magnetic Surfaces, Thin Films, and Multilayers*, edited by S.S.P. Parkin, H. Hopster, J.P. Renard, T. Shinjo, and W. Zinn, MRS Symposia Proceedings No. 231 (Materials Research Society, Pittsburgh, 1992), p. 211.
¹²W.F. Egelhoff, Jr. and M.T. Kief, Phys. Rev. B **45**, 7795 (1992).
¹³J. Kohlhepp *et al.*, J. Magn. Magn. Mater. **111**, L231 (1992).
¹⁴J.P. Renard *et al.*, J. Magn. Magn. Mater. **115**, L147 (1992).
¹⁵S.S.P. Parkin *et al.*, Phys. Rev. B **46**, 9262 (1992).
¹⁶D. Greig *et al.*, J. Magn. Magn. Mater. **110**, L239 (1992).
¹⁷P. Bödeker *et al.*, Phys. Rev. B **47**, 2353 (1993).
¹⁸K. Bröhl *et al.*, J. Cryst. Growth **127**, 682 (1993).
¹⁹C.F. Majkrzak, Physica B **173**, 75 (1991).
²⁰A. Schreyer *et al.*, J. Appl. Phys. (to be published).
²¹N. Metoki *et al.*, J. Magn. Magn. Mater. **118**, 57 (1993).
²²J.F. Ankner *et al.*, in *Magnetic Ultrathin Films, Multilayers, and Surfaces*, edited by C. Chappert, R. Clarke, R.F.C. Farrow, P. Grünberg, W.J.M. de Jonge, B.T. Jonker, Kanan M. Krishnan, and Shigeru Tsunashima, MRS Symposia Proceedings (Materials Research Society, Pittsburgh, in press); for a general description see J.F. Ankner and C.F. Majkrzak, in *Neutron Optical Devices and Applications*, edited by C.F. Majkrzak and J.L. Wood, SPIE Conference Proceedings Vol. 1738 (SPIE, Bellingham, WA, 1992), pp. 260-269.
²³C. Dupas *et al.* (unpublished).
²⁴R. Miranda (private communication).